The Theoretical Description for the Use of Poly(7-hydroxyphenoxazone) as Electrode Modifier for pH Monitoring

Volodymyr V. Tkach [1,*] , **Tetiana V. Morozova** [2] , **Andrii O. Hlukhonets** [2] , **Marta V. Kushnir** [1] ,

Sílvio C. de Oliveira [3] , **Viktor V. Kryvetskyi** [4] , **Inna I. Kryvetska** [4] , **Igor V. Kryvetskyi** [4] ,

Igor G. Biryuk [4] , **Tetiana B. Sykyrytska** [4] , **Yana G. Ivanushko** [4] , **Maryna G. Besplitnik** [4] ,

Petro I. Yagodynets [1,*] , **Adriano O. da Silva** [5] , **Jarem R. Garcia** [6] ,

José Inácio Ferrão da Paiva Martins [7] , **Gennadii F. Tkach** [8] , **Oleg P. Melnyk** [8] ,

Oleksii O. Melnyk [8] , **Maria V. Melnyk** [8] , **Maria João Monteiro** [9] , **Lilia O. Nikitchenko** [10] ,

Iryna G. Patseva [11] , **Vitalina Lukyanova** [11] , **Liudmyla Mohelnytska** [11] , **Mykola P. Krasko** [12] ,

Vira M. Odyntsova [12]

[1]   Chernivtsi National University, 58001, Kotsyubynsky Str. 2, Chernivtsi, Ukraine
[2]   National Transport University, 02000, Omelianovych-Pavlenko Str. 1, Kyiv, Ukraine
[3]   Institute of Chemistry. Federal University of Mato Grosso do Sul, 79074 – 460, Av. Sen. Felinto Müller, 1555, Vila Ipiranga, Campo Grande, MS, Brazil
[4]   Bukovinian State Medical University, 58001, Teatralna Sq, 9, Chernivtsi, Ukraine
[5]   Federal University of the West of Pará, Juruti Campus, 68170 – 000, Rua Veríssimo de Souza Andrade, s/n, Juruti, PA, Brazil
[6]   State University of Ponta Grossa, Uvaranas Campus, Av. Gal. Carlos Cavalcanti, 4748, 84030-900, Ponta Grossa, PR, Brazil
[7]   Engineering Faculty of the University of Porto, 4200-465, Rua Dr. Roberto Frias, s/n, Porto, Portugal
[8]   National University of Life and Environmental Science of Ukraine, 03041, Heroiv Oborony Str, 15, Kyiv, Ukraine
    University of Trás-os-Montes and Alto Douro, Quinta de Prados, 5001-801, Folhadela, Vila Real, Portugal
[9]   Vinnytsia State Pedagogical University, 21000, Ostroz'ky Str. 32, Vinnytsia, Ukraine
[10] Zhytomyr Polytechnic State University, 10005, Chudnivs'ka Str. 103, Zhytomyr, Ukraine
[11] Zaporizhzhia State University of Medicine and Pharmacy, 69600, Mayakovsky Ave. 24, Zaporizhzhia, Ukraine
*   Correspondence: nightwatcher2401@gmail.com (V.V.T.), ved1988mid@rambler.ru (P. I.Y.) ;

Abstract: The possibility of electroanalytical variation for a well-known litmus acidity test has been evaluated theoretically. In this system, pH is measured by a carbon material electrode, modified by the electropolymerized 7-hydroxyphenoxazone – the most pH-sensitive litmus dye. The investigation of the correspondent mathematical modeling confirms that the poly(7-hydroxyphenoxazone)-modified cathode is suitable for the pH measurements, especially in neutral and acidic solutions. Although the oscillatory and monotonic instabilities are more probable than in similar systems, the electroanalytical process tends to be efficient, and the analytical signal is easy to interpret.

1. Introduction

The litmus test is one of the first used to monitor the acidity and basicity of the solutions [1–4]. Litmus, found in lichens, growing all over the world, including those of the gene *Rocella, Lecanora, Ochrolechia, Parmotrema, Dendrographa,* and *Palmotrema* generally contain litmus dyes, which include both carbo and heterocyclic compounds.

The main litmus chromophore is 7-hydroxyphenoxazone (Figure 1) [5–6], which is violet in a neutral medium, furtherly becoming red in acidic solutions and blue in basic ones:
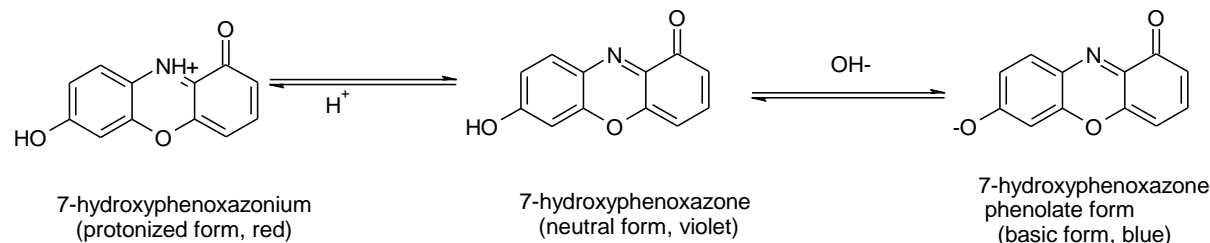

7-hydroxyphenoxazonium
(protonized form, red)

7-hydroxyphenoxazone
(neutral form, violet)

7-hydroxyphenoxazone
phenolate form
(basic form, blue)

Figure 1. 7-hydroxyphenoxazone and litmus colors.

Dye electropolymerization become a popular and efficient tool for electroanalytical processes [7–14]. In these systems, dye polymers become efficient active substances and mediators for the electroanalysis of different analytes. Moreover, in the case of poly(7-hydroxyphenoxazone)-assisted pH sensing, it will become a modernized version of a known method. Considering the presence of accepting groups in the dye structure, the cathodic pH measurement becomes viable.

Nevertheless, the presence of electrochemical instabilities, which make the analytical signal difficult to interpret, may be associated with different behaviouristic effects of the electroanalytical processes [15–17]. Those instabilities are typical and may limit the electroanalytical and removal use of the electrochemical process. To foresee the possibility of the realization of the electrochemical instabilities, like the effect they may produce, it´s necessary to investigate the process from the mechanical point of view and analyze its behavior theoretically.

So, the goal of this work is the mechanistic evaluation for poly(7-hydroxyphenoxazone)-assisted reductive pH measurement, in which the dye interaction with protons with further reduction is included. The correspondent mathematical model is developed and analyzed using linear stability theory and bifurcation analysis. The theoretical investigation includes comparing the behavior of this system with that of similar ones [18–24].

2. Materials and Methods

The first stage of the electroanalytical process includes the pyridinic nitrogen protonation, yet described in Figure 1 as one yielding the red (acidic) litmus form. In the case of cathodic reduction, the 7-hydroxyphenoxazonium salt is thereby reduced by either protonated pyrizinic nitrogen or carbonyl moiety.

The protons are involved in all the mentioned processes, which is why both electrochemical peaks may be used for pH measurement. Depending on the electropolymerization technique, the 7-hydroxyphenoxazone units may be joined via each unit's electrophilic and nucleophylic sites (Figure 2).
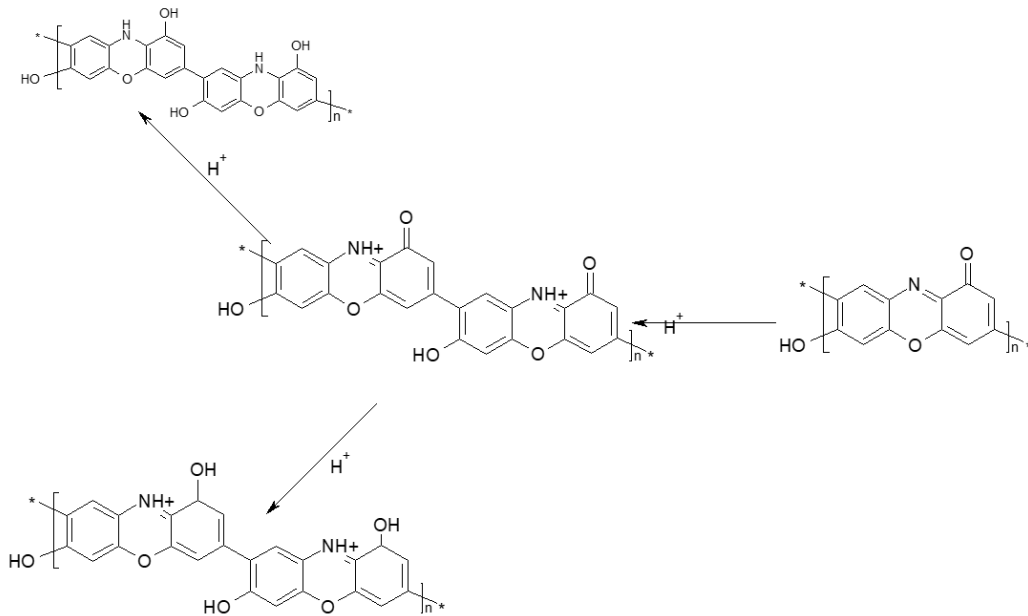
Figure 2. The scheme for electroanalytical process.

Taking this into account and accepting certain assumptions [18–21], we describe the system´s behavior by a bivariant equation set, exposed as:

$$\begin{cases} \frac{dh}{dt} = \frac{2}{\delta}\left(\frac{H}{\delta}(h_0 - h) - r_1 - r_{21} - r_{22}\right) \\ \frac{dp}{dt} = \frac{1}{P}(r_1 - r_{21} - r_{22}) \end{cases} \quad (1)$$

Herein, h is the proton pre-surface concentration, H is its diffusion coefficient, h_0 is the protons' bulk concentration, p is the protonated polymer surface coverage degree, P is its maximal surface concentration, and the parameters r stand for the correspondent reaction rates, calculated as:

$$r_1 = k_1(1 - p)h^n \exp(-\alpha h) \quad (2)$$

$$r_{21} = k_{21}ph^x \exp\left(-\frac{mF\varphi_0}{RT}\right) \quad (3)$$

$$r_{22} = k_{22}ph^y \exp\left(-\frac{nF\varphi_0}{RT}\right) \quad (4)$$

Herein, the parameters k stand for the correspondent reaction rate constants, n is the number of monomer units, α is the parameter relating the pH and DEL ionic force, x and y are the proton reaction orders in the electrochemical stages, m and n are the numbers of the transferred electrons, F is the Faraday number, φ_0 is the zero-charge-related potential slope, R is the universal gas constant, and T is the absolute temperature.

The ionic substances and forms are highly involved in all the chemical and electrochemical stages, which is why the DEL-reñated oscillatory behavior becomes more probable than for the simplest case. Nevertheless, the poly(7-hydroxyphenoxazone)-assisted pH electrochemical monitoring by cathodic route is efficient, especially in acidic and neutral media, as shown below.

3. Results and Discussion

In order to investigate the electrochemical behavior of the system with the poly(7-hydroxyphenoxazone)-assisted pH electrochemical determination, we analyze the equation-set (1) alongside the algebraic relations (2–4) by means of linear stability theory. The steady-state Jacobian matrix members may be described as (5):

$$\begin{pmatrix} a_{11} & a_{12} \\ a_{21} & a_{22} \end{pmatrix} \qquad (5)$$

in which:

$$a_{11} = \frac{2}{\delta}\left(-\frac{H}{\delta} - nk_1(1-p)h^{n-1}\exp(-\alpha h) + \alpha k_1(1-p)h^n\exp(-\alpha h) - \right.$$

$$\left. xk_{21}ph^{x-1}\exp\left(-\frac{mF\varphi_0}{RT}\right) - yk_{22}ph^{y-1}\exp\left(-\frac{nF\varphi_0}{RT}\right)\right) \qquad (6)$$

$$a_{12} = \frac{2}{\delta}\left(k_1 h^n\exp(-\alpha h) - k_{21}h^x\exp\left(-\frac{mF\varphi_0}{RT}\right) - k_{22}ph^y\exp\left(-\frac{nF\varphi_0}{RT}\right) + \right.$$

$$\left. j\left(k_{22}ph^y\exp\left(-\frac{nF\varphi_0}{RT}\right) + k_{22}ph^y\exp\left(-\frac{nF\varphi_0}{RT}\right)\right)\right) \qquad (7)$$

$$a_{21} = \frac{1}{P}\left(nk_1(1-p)h^{n-1}\exp(-\alpha h) - \alpha k_1(1-p)h^n\exp(-\alpha h) - \right.$$

$$\left. xk_{21}ph^{x-1}\exp\left(-\frac{mF\varphi_0}{RT}\right) - yk_{22}ph^{y-1}\exp\left(-\frac{nF\varphi_0}{RT}\right)\right) \qquad (8)$$

$$a_{22} = \frac{1}{P}\left(-k_1 h^n\exp(-\alpha h) - k_{21}h^x\exp\left(-\frac{mF\varphi_0}{RT}\right) - k_{22}ph^y\exp\left(-\frac{nF\varphi_0}{RT}\right) + \right.$$

$$\left. j\left(k_{22}ph^y\exp\left(-\frac{nF\varphi_0}{RT}\right) + k_{22}ph^y\exp\left(-\frac{nF\varphi_0}{RT}\right)\right)\right) \qquad (9)$$

Avoiding the cumbersome expressions, we introduce new variables, rewriting the determinant as (10)

$$\frac{2}{\delta P}\begin{vmatrix} -\kappa - Y - Z & \Lambda - \Omega \\ Y - Z & -\Lambda - \Omega \end{vmatrix} \qquad (10)$$

The main conditions of the steady-state stability and the essential instabilities are exposed in Table 1:

Table 1. The main stability conditions for the bivariant equation sets.

Singular point	Requirement
Steady-state stability	Tr J < 0, Det J>0
Oscillatory instability (Hopf bifurcation)	Tr J = 0, Det J>0
Monotonic instability (Saddle-node bifurcation)	Tr J < 0, Det J>0

Considering the elements (6) and (9), this system's oscillatory behavior can appear. The main Hopf bifurcation condition is realized if the main diagonal contains positive elements related to the positive callback.

The realization of the oscillatory behavior by Hopf bifurcation is given by the presence of the positive elements in the matrix main diagonal (which is necessary to satisfy the main condition Tr J=0). These elements are: $\alpha k_1(1-p)h^n\exp(-\alpha h) > 0$ if $\alpha>0$ and $j\left(k_{22}ph^y\exp\left(-\frac{nF\varphi_0}{RT}\right) + k_{22}ph^y\exp\left(-\frac{nF\varphi_0}{RT}\right)\right) > 0$, if j>0. This positivity defines the oscillatory behavior caused by the capacitance effect of DEL in the electrochemical (in the case of the positivity of j) and chemical (in the case of the positivity of a) stages. The oscillation frequency and amplitude depend on the global electrolyte ionic composition. Mathematically, the condition of the oscillatory behavior will be described as (11):

$$\begin{cases} -\frac{2}{\delta}(\kappa + Y + Z) - \frac{1}{P}(\Lambda + \Omega) = 0 \\ \frac{2}{\delta P}(\kappa\Lambda + \kappa\Omega + 2Y\Omega + 2Z\Lambda) > 0 \end{cases} \qquad (11)$$

In the case of the negativity of these elements, steady-state stability is warranted. Its condition will be described as (12):

$$\begin{cases} -\frac{2}{\delta}(\kappa + Y + Z) - \frac{1}{P}(\Lambda + \Omega) < 0 \\ \frac{2}{\delta P}(\kappa\Lambda + \kappa\Omega + 2Y\Omega + 2Z\Lambda) > 0 \end{cases} \qquad (12)$$

Really, if the variables a and j have null or negative values, the left side of the first inequation of (12) will be more damaging, stabilizing the system and ensuring the efficiency of the process from both electroanalytical and removal points of view. From the electroanalytical point of view, this condition will define the linear dependence between the electrochemical parameter and concentration, providing a straightforward interpretation of the analytical signal. As for the process, it will be kinetically controlled, considering rapid proton diffusion in water solutions.

As for the detection limit, it is correspondent to the monotonic instability, defined by the condition of Det J=0, or (13):

$$\begin{cases} -\frac{2}{\delta}(\kappa + Y + Z) - \frac{1}{P}(\Lambda + \Omega) < 0 \\ \frac{2}{\delta P}(\kappa\Lambda + \kappa\Omega + 2Y\Omega + 2Z\Lambda) = 0 \end{cases} \qquad (13)$$

The margin between the stable, steady, and unstable states is formed at this point. A multiplicity of unstable steady-states corresponds to this margin. The system chooses one of them, which is destroyed if the system conditions change.

The pOH measurement in an alkaline medium is also possible over poly(7-hydroxyphenoxazone). It will be manifested as an anodic process in which the *ortho*-penalization, followed by quinone-hydroquinone oxidation, is realized. In this case, the system's behavior will be described by a trivariate equation set (14):

$$\begin{cases} \frac{da}{dt} = \frac{2}{\delta}\left(\frac{A}{\delta}(a_0 - a) - r_1\right) \\ \frac{dp}{dt} = \frac{1}{P}(r_1 - r_2) \\ \frac{dp*}{dt} = \frac{1}{P}(r_2 - r_{31} - r_{32}) \end{cases} \qquad (14)$$

Which will be evaluated in our next works.

4. Conclusions

From the behavior investigation of the system with the pH electrochemical detection and monitoring, assisted by a conducting polymer based on litmus main chromophore, it was possible to conclude that the polyphenolic conducting polymer, based on a natural source, may be an efficient cathode modifier for pH determination, especially in neutral and acidic media. The behavior of the process becomes more accomplished due to the presence of the ionic form transformations, enhancing the probability of the oscillatory behavior. Nevertheless, it is an efficient process controlled by the kinetics of the chemical and electrochemical reactions that make up part of it.

Conflicts of Interest

The authors declare no conflict of interest.

References

1. Rezaeivala, M.; Bozorg, M.; Rafiee, N.; Sayin, K.; Tuzun, B. Corrosion inhibition of Carbon Steel using a new morpholine-based ligand during acid pickling: Experimental and theoretical studies. *Inorg. Chem. Commun.* **2023**, *148*, 110323, https://doi.org/10.1016/j.inoche.2022.110323.

2. Zhu, S.; Sun, B.; Chen, Y.; Li, T.; Zhou, G.; Zhao, H.; Mao, W.; Zhao, Y. An excellent pH-controlled resistive switching memory device based on self-colored $(C_7H_7O_4N)_n$ extracted from a lichen plant. *J. Mater. Chem. C* **2019**, *7*, 7593-7600, https://doi.org/10.1039/c8tc06207B.

3. Almasi, H.; Forghani, S.; Moradi, M. Recent advances on intelligent food freshness indicators; an update on natural colorants and methods of preparation. *Food Packag. Shelf Life* **2022**, *32*, 100839, https://doi.org/10.1016/j.fpsl.2022.100839.

4. Yin, J.; Li, J.; Reddy, V.S.; Ji, D.; Ramakrishna, S.; Xu, L. Flexible Textile-Based Sweat Sensors for Wearable Applications. *Biosensors* **2023**, *13*, 127, https://doi.org/10.3390/bios13010127.

5. Bordbar, M.M.; Sheini, A.; Hashemi, P.; Hajian, A.; Bagheri, H. Disposable Paper-Based Biosensors for the Point-of-Care Detection of Hazardous Contaminations–A Review. *Biosensors* **2021**, *11*, 316, https://doi.org/10.3390/bios11090316.

6. Bilgen, E.; Suvacı, Z.; Çetinkol, Ö.P.; Forough, M. 26 - Disposable paper-based sensors. In Fundamentals of Sensor Technology; Barhoum, A., Altintas, Z., Eds.; Woodhead Publishing, **2023**; 803-860, https://doi.org/10.1016/B978-0-323-88431-0.00028-4.

7. Tkach, V.V.; Martins, J.I.F.d.P.; Ivanushko, Y.G.; Yagodynets', P.I. Dye Electropolymerization for Electrochemical Analysis. A Brief Review. *Biointerface Res. Appl. Chem.* **2022**, *12*, 4028-4047, https://doi.org/10.33263/BRIAC123.40284047.

8. Liv, L. A facile poly(allura red) film for signal-amplified electrochemical sensing of dopamine and uric acid in human plasma and urine. *Microchem. J.* **2023**, *195,* 109425, https://doi.org/10.1016/j.microc.2023.109425.

9. Porfireva, A.; Plastinina, K.; Evtugyn, V.; Kuzin, Y.; Evtugyn, G. Electrochemical DNA Sensor Based on Poly(Azure A) Obtained from the Buffer Saturated with Chloroform. *Sensors* **2021**, *21*, 2949, https://doi.org/10.3390/s21092949.

10. Sugiyama, K.; Watanabe, K.; Komatsu, S.; Yoshida, K.; Ono, T.; Fujimura, T.; Kashiwagi, Y.; Sato, K. Electropolymerization of Azure A and pH Sensing Using Poly(Azure A)-modified Electrodes. *Anal. Sci.* **2021**, *37*, 893–896, https://doi.org/10.2116/analsci.20P341.

11. Tkach, V.V.; Kushnir, M.V.; Kopiika, V.V.; Luganska, O.V.; Omelianchyk, L.O.; Yeshchenko, Y.V.; Kormosh, Z.O.; Kryvetskyi, V.V.; Kryvetskyi, I.V.; Kryvetska, I.I.; Rusnak, V.F.; Banul, B.Y.; Gordiyenko, N.M.; Britsyna, Y.V.; Bagrii, K.L.; Strutynska, L.T.; Danyliuk, I.P.; De Oliviera, S.C.; Yagodynets, P.I.; Razhabova, D.B.; Niyazov, L.N. Theoretical Evaluation for the Assisted Electropolymerization of a Monomer, Obtained by an Indirect Electrochemical Synthesis. *Lett. Appl. NanoBioSci.* **2022**, *11*, 3605-3610, https://doi.org/10.33263/LIANBS112.36053610.

12. Zhang, Y.; Huang, R.; Wang, X.; Wang, Z.; Song, B.; Du, Y.; Lu, Q.; Chen, X.; Sun, J. Facile large-scale preparation of vanadium pentoxide -polypyrrole composite for aqueous zinc-ion batteries. *J. Alloys Compd.* **2022**, *907*, 164434, https://doi.org/10.1016/j.jallcom.2022.164434.

13. Chavan, U.D.; Prajith, P.; Kandasubramanian, B. Polypyrrole based cathode material for battery application. *Chem. Eng. J. Adv.* **2022**, *12*, 100416, https://doi.org/10.1016/j.ceja.2022.100416.

14. Kondratiev, V.; Holze, R. Intrinsically Conducting Polymer Binders for Battery Electrodes. *Encyclopedia* **2022**, *2*, 1753-1762, https://doi.org/10.3390/encyclopedia2040120.

15. Chepurnaya, I.; Smirnova, E.; Karushev, M. Electrochemically Active Polymer Components in Next-Generation $LiFePO_4$ Cathodes: Can Small Things Make a Big Difference?. *Batteries* **2022**, *8*, 185, https://doi.org/10.3390/batteries8100185.

16. Dong, R.; Zhang, T.; Liu, J.; Li, H.; Hu, D.; Liu, X.; Xu, Q. Mechanistic Insight into Polypyrrole Coating on V_2O_5 Cathode for Aqueous Zinc-Ion Battery. *ChemElectroChem* **2022**, *9*, e202101441, https://doi.org/10.1002/celc.202101441.

17. Das, I.; Goel, N.; Gupta, S.K.; Agrawal, N.R. Electropolymerization of pyrrole: Dendrimers, nano-sized patterns and oscillations in potential in presence of aromatic and aliphatic surfactants. *J. Electroanal. Chem.* **2012**, *670*, 1-10, https://doi.org/10.1016/j.jelechem.2012.01.023.

18. Aoki, K.; Mukoyama, I.; Chen, J. Competition between Polymerization and Dissolution of Poly(3-methylthiophene) Films. *Russ. J. Electrochem.* **2004**, *40*, 280-285, https://doi.org/10.1023/B:RUEL.0000019665.59805.4c.

19. Tkach, V.V.; Kushnir, M.V.; Storoshchuk, N.M.; de Oliveira, S.C.; Luganska, O.V.; Kopiika, V.V.; Novosad, N.V.; Lukanova, S.M.; Ivanushko, Y.G.; Ostapchuk, V.O.; Melnychuk, S.P.; Yagodynets', P.I.; de Paiva Martins, J.I.F.; dos Reis, L.V. O uso do hidróxido de vanádio bivalente para a eliminação da sucralose das águas naturais e de esgoto da indústria alimentar e farmacêutica. Uma avaliação teórica. *Rev. Colomb. Cienc. Quím. Farm.* **2023**, *52*, 348–361, https://doi.org/10.15446/rcciquifa.v52n2.110749.

20. Akinay, Y.; Çolak, B.; Turan, M.E.; Akkuş, I.N.; Kazici, H.Ç.; Kizilçay, A.O. The electromagnetic wave absorption properties of woven glass fiber composites filled with Sb_2O_3 and SnO_2 nanoparticles doped mica pigments. *Polym. Compos.* **2022**, *43*, 8784–8794, https://doi.org/10.1002/pc.27061.

21. Pinyou, P.; Blay, V.; Monkrathok, J.; Janphuang, P.; Chansaenpak, K.; Pansalee, J.; Lisnund, S. A facile method for generating polypyrrole microcapsules and their application in electrochemical sensing. *Microchim. Acta.* **2022**, *189,* 410, https://doi.org/10.1007/s00604-022-05512-1.

22. Karataş, Y.; Çetin, T.; Akinay, Y.; Gülcan, M. Synthesis and characterization of Pd doped MXene for hydrogen production from the hydrolysis of methylamine borane: Effect of cryogenic treatment. *J. Energy Inst.* **2023**, *109,* 101310, https://doi.org/10.1016/j.joei.2023.101310.

23. Habibi, M.; Habibi-Yangjeh, A.; Akinay, Y.; Khataee, A. Oxygen vacancy-rich CeO_2 decorated with Cu_3BiS_3 nanoparticles: Outstanding visible-light photocatalytic performance towards tetracycline degradation. *Chemosphere* **2023**, *340*, 139828, https://doi.org/10.1016/j.chemosphere.2023.139828.

24. Yigit, A.; Pınar, P.T.; Akinay, Y.; Alma, M.H.; Menges, N. Nanotube-Boramidic Acid Derivative for Dopamine Sensing. *ChemistrySelect* **2021**, *24*, 6302-6313, https://doi.org/10.1002/slct.202101316.